Observation-based Blended Projections from Ensembles of Regional Climate Models

Esther Salazar, Dorit Hammerling, Xia Wang, Bruno Sansó, Andrew O. Finley, and Linda Mearns *

December 20, 2013

Abstract

We consider the problem of projecting future climate from ensembles of regional climate model (RCM) simulations using results from the North American Regional Climate Change Assessment Program (NARCCAP). To this end, we develop a hierarchical Bayesian space-time model that quantifies the discrepancies between different members of an ensemble of RCMs corresponding to present day conditions, and observational records. Discrepancies are then propagated into the future to obtain high resolution blended projections of 21st century climate. In addition to blended projections, the proposed method provides location-dependent comparisons between the different simulations by estimating the different modes of spatial variability, and using the climate model-specific coefficients of the spatial factors for comparisons. The approach has the flexibility to provide projections at any spatial scale of potential interest to stakeholders while correctly accounting for the uncertainties associated with projections at that scale. We demonstrate the methodology with simulations from WRF using three different forcings: NCEP, CCSM and CGCM3. We use simulations for two time periods: current climate conditions, covering 1971 to 2000, and future climate conditions under the SRES A2 emissions scenario, covering 2041 to 2070. We investigate and project yearly mean summer and winter temperatures for a domain in the South West of the United States.

*Esther Salazar is Assistant Research Professor, Department of Electrical and Computer Engineering, Duke University (esther.salazar@duke.edu); Dorit Hammerling is Postdoctoral Associate at the National Center for Atmospheric Research (dorith@ucar.edu) and Department of Statistics, University of Washington; Xia Wang is Assistant Professor, Department of Mathematical Sciences, University of Cincinnati, (wang2x7@UCMAIL.UC.EDU); Bruno Sansó is Professor and Chair, Department of Applied Mathematics and Statistics, University of California Santa Cruz (bruno@ams.ucsc.edu); Andrew O. Finley is Associate Professor, Departments of Forestry and Geography, Michigan State University (finleya@msu.edu); Linda Mearns is Senior Scientist at the National Center for Atmospheric Research, (lindam@ucar.edu)

1 Introduction

The idea of assessing the uncertainty in future climate predictions using multi-model ensembles is at the core of the World Climate Research Program (WCRP) Coupled Model Intercomparison Project Phases 3 and 5 (CMIP3, CMIP5) (Meehl et al., 2007; Taylor et al., 2012). A fundamental difficulty of such assessments, as argued in Tebaldi et al. (2011), is that the internal variability of the climate system can overwhelm the variability that is due to external forcings. Thus, two models with similar structural responses, may produce simulations for a given time and location that provide conflicting information. For this reason, we adopt a probabilistic approach to address multi-model ensembles. This is based on the assumption that a given simulation from a climate model is a sample from a distribution of climates. Similarly, observational records are viewed as samples and provide noisy information about the climate.

More specifically, in the approach considered in this paper, simulations from a given climate model are assumed to correspond to an unobserved underlying state plus a model dependent discrepancy. Observational records are assumed to provide information about the same underlying state, and are subject to observational error. Quantifying model discrepancies is key to obtaining unified estimates of the underlying state. It also allows for the assessment of the different models under consideration. Regional climate models produce simulations that have high spatial resolution. To produce an estimation of model discrepancies that focuses on relevant spatial features, rather than high resolution details, Salazar et al. (2011) consider projections onto the main modes of spatial variability. In this paper we follow the same approach. We use a common set of basis functions for all the spatial fields. The bases depend on parameters that are estimated using all sources of information, incorporating all uncertainties in the data. We obtain spatially-varying discrepancies for each member of the multi-model ensemble. These are subsequently used to obtain high resolution unified climate projections. Our method has the flexibility of providing results at any spatial scale with rigorously derived uncertainties corresponding to that scale. This is an important feature for stakeholders with interest in, for example, irregular domains such as watershed managers. Moreover, our Bayesian approach provides a probabilistic quantification of all the uncertainties relevant to the output.

Following the framework of rigorous statistical methods for climate model analysis, like the ones in Tebaldi and Sansó (2008); Smith et al. (2009); Rougier et al. (2010), we use hierarchical models to blend information from historical records and multi-model simulation ensembles. Hierarchical models (see, for example, Cressie and Wikle, 2011), split the variability of an observed system in three clearly defined levels of conditional probabilities. The first level corresponds to the observational model. The second level to the underlying process, and the third level informs the learning of the parameters in the previous two levels. This setting is intrinsically Bayesian. That is, it lends itself naturally to inferential methods that use probability to quantify uncertainties for all unknown quantities in a model. A summary of the information in all three levels of the model is provided by the "posterior distribution." This corresponds to the distribution of all unobserved quantities, conditional on the observed ones. The Bayesian framework allows uncertainty to be propagated through

the hierarchical levels to the posterior distribution of model parameters and predictions.

To illustrate our methods we use simulations from the North American Regional Climate Change Assessment Program (NARCCAP) (Mearns et al., 2009) (`www.narccap.ucar.edu`). This is an international program to produce high resolution climate simulations to assess climate change on a regional level. The goal of the project is to investigate the uncertainty of future climate projections at a regional level. NARCCAP covers all of North America and part of the Caribbean with a resolution of 50km. It involves a number of combinations of six different RCMs and four different atmosphere-ocean coupled general circulation models (AOGCMs), in a way that each RCM is run with boundary conditions given by two different AOGCMs. The AOGCMs have been forced with the SRES A2 emissions scenario for the 21st century, thereby eliminating any differences in assumed emissions among the model runs. In summary, NARCCAP is a carefully designed experiment to assess the variability of RCMs. As a byproduct, the project provides a set of multi-model ensembles of simulations at a regional level for current and future climates. We use a subset of these ensembles to demonstrate the methodology proposed in this paper.

2 Data

We use simulations from one of the RCMs included in the NARCCAP program, the Weather Research & Forecasting regional model (WRF) driven by different boundary conditions. WRF is a next-generation mesoscale numerical weather prediction model maintained by NCAR. The three boundary conditions to drive the WRF model (within NARCCAP) are the National Centers for Environmental Modeling (NCEP) reanalysis, the Community Climate System Model (CCSM) and the Third Generation Coupled Global Climate Model (CGCM3). The NCEP reanalysis is based on various sources of observed data and an atmospheric model. The version "NCEP-2" is used by NARCCAP. CCSM is a coupled GCM developed by the University Corporation for Atmospheric Research (UCAR) with funding from the National Science Foundation (NSF), Department of Energy (DOE), and NASA. CCSM is maintained by the National Center for Atmospheric Research (NCAR). CGCM3 is a coupled GCM developed by the team at the Canadian Centre for Climate Modelling and Analysis (CCCma). Details of these models are available on the NARCCAP website (`www.narccap.ucar.edu`) and the references therein. Simulations with forcings from WRF+CCSM and WRF+CGCM3 show distinct trends and patterns compared to other RCM and GCM combinations included in the NARCCAP program, which are more uniform (for example the simulations chosen by Salazar et al. (2011)). The presence of these distinct features highlights the ability of the presented statistical model to account for these discrepancies in forecasting 21st century climate.

NARCCAP simulations cover the years of 1971-2000 for the current period and 2041-2070 for the future scenario. These data are available at 3 hour and daily intervals. In an initial phase, simulations were obtained for 1979-2004 using NCEP boundary conditions. Observational data for the current period, 1971–2010, were created using data from the National Oceanic and Atmospheric Administration (NOAA) Integrated Surface Database

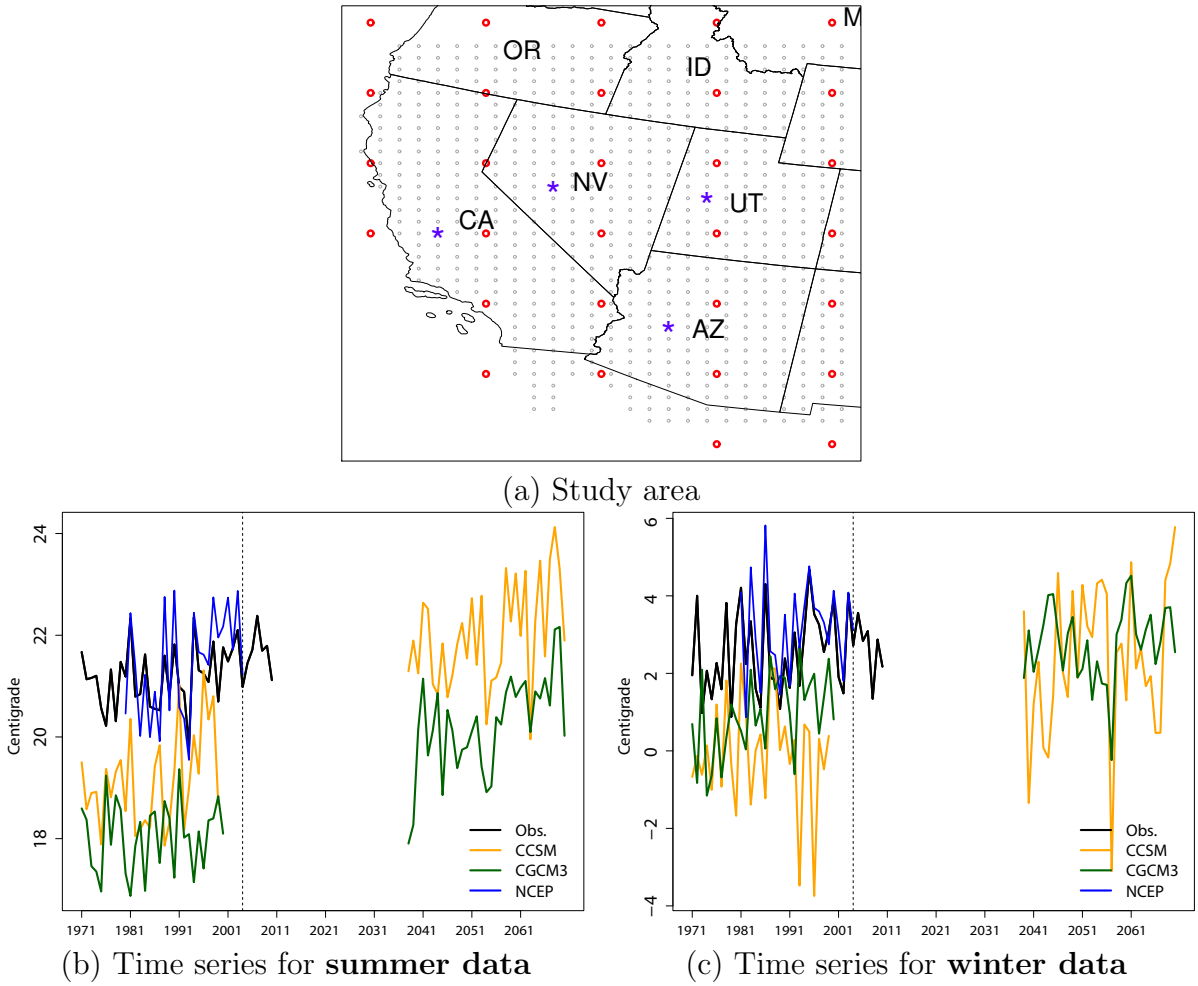

(a) Study area

(b) Time series for **summer data**

(c) Time series for **winter data**

Figure 1: (a) Study area: the fine grid corresponds to the resolution of the RCM output (resolution 50 km), the coarse grid corresponds to the selected knots (resolution 300 km), and the blue stars to selected prediction locations. (b)-(c) Time series of summer and winter mean temperature for spatially averaged data.

(ISD; `www.ncdc.noaa.gov/oa/climate/isd`). Thus, 1971–2010 and 2041–2070 are the time periods that we consider in this paper. Regarding the spatial domain, we focus on the south-west region of the United States depicted in Figure 1 (a). We consider summer and winter mean temperature for the observational record, and RCM simulations with three forcings discussed above. The time frame for summer is June 21 – September 21 and for winter is December 21 – March 21. Panels (b) and (c) in Figure 1 show the spatially averaged time series of the different data sources. Figure 2 shows the spatial distribution of temperature under present conditions, according to the four different data sources, for summer and winter. The study area includes a total of 713 grid points.

In order for the observations to share a common map projection with the RCM data, the

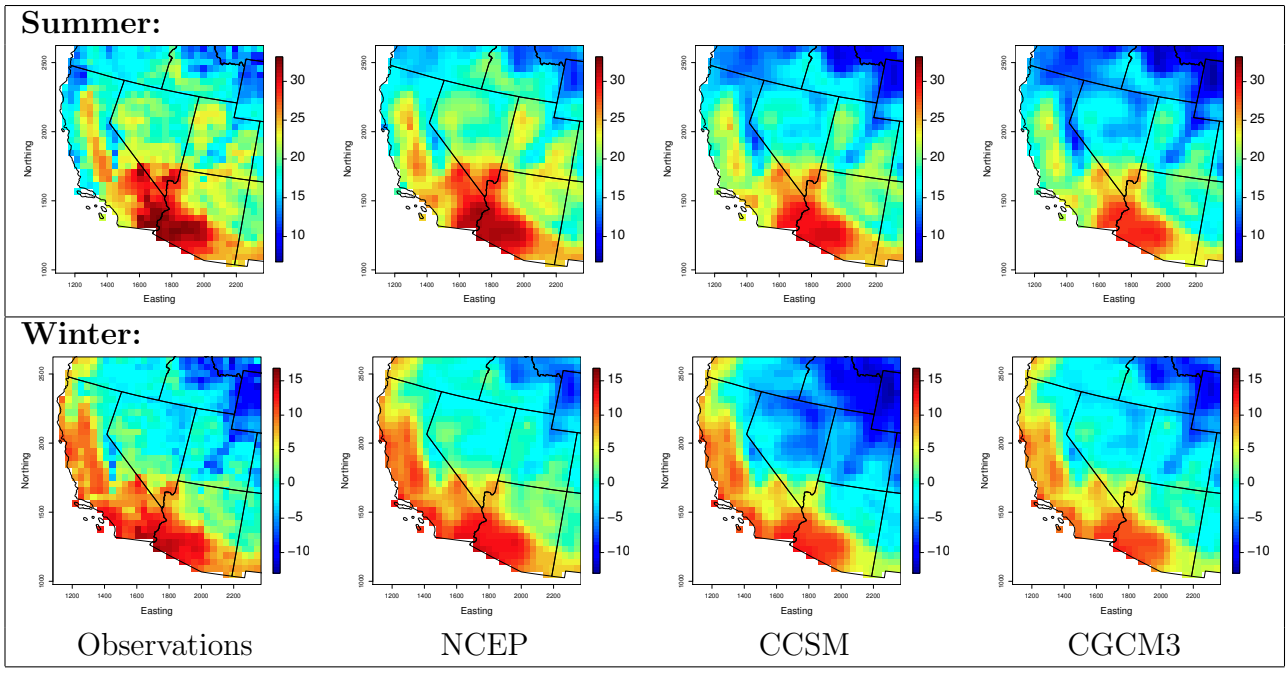

Figure 2: Temporal average of the observations (1st column), NCEP (2nd column), and simulations based on CCSM (3rd column) and CGCM3 (4th column) averaged over the periods 1980–1999 (for summer) and 1981–1999 (for winter). Temperature values are in °C.

ISD data coordinates were reprojected from latitude and longitude into Lambert conformal conic. Temperature predictions at each RCM pixel centroid (fine gray grid in Figure 1 (a)) were made using the ISD 3-hour weather station data and a spatial regression model that included an intercept, elevation as a covariate, spatial random effects, and a nugget. The spatial random effects followed a zero centered Gaussian process with an exponential spatial covariance function. Model parameters were estimated simultaneously using maximum likelihood. These 3-hour predictions were then averaged to create estimates of yearly mean summer and winter temperature.

3 Methods

Given the different nature of the variability in observational records and simulations, we use assessment methods that relay on broad spatial and temporal patterns. Our approach considers baselines that are common to all compared models. Thus, following Beltrán et al. (2012), we seek to extract large scale spatial features from spatio-temporal fields. This can be conveniently achieved by representing such fields using a set of basis functions. Following such approach, a space-time field indexed in time t and space $\boldsymbol{s}$, say $y_t(\boldsymbol{s})$, is represented by

a linear combination of spatially-varying functions, say $\Psi_i(\boldsymbol{s})$, yielding the expression

$$y_t(\boldsymbol{s}) = \sum_{i=1}^{\infty} \Psi_i(\boldsymbol{s})\alpha_i(t) \quad . \tag{1}$$

The functions $\Psi_i(\boldsymbol{s})$ summarize the main patterns of spatial variability of the field. Such patterns are weighed in a time-varying fashion by the coefficients $\alpha_i(t)$. In order to assess the differences between a number of space-time fields, like the ones that result from a multi-model ensemble of climate model simulations, we represent all of them on a common basis set. We can then compare the different time-varying coefficients associated with each ensemble member and each mode of spatial variability, as captured by each basis function. Empirical orthogonal functions (EOF, see, for example, Hannachi et al., 2007) are a popular method to obtain a set of basis functions. These are obtained from a principal component analysis of the covariance matrix, which is empirically estimated from the observations. Hannachi et al. (2007) discuss a number of shortcomings of EOFs that have prompted elaborations and extensions of the method. The application of those methods is not immediate in our setting. In fact it is not clear how to combine the information from different sets of simulations to produce empirical estimates of the basis functions. Our approach is based on assuming the existence of a common underlaying Gaussian process. Such a process induces a set of common basis functions. Inference is performed using a hierarchical model.

A detailed description of the methods used in this paper is presented in Salazar et al. (2011). Here we describe the most important features of the statistical model. Let $y_t(\boldsymbol{s})$ be the observed temperatures at time t and location $\boldsymbol{s}$ and $y_{tj}^{CM}(\boldsymbol{s})$ be the RCM output using NCEP ($j = 1$), CCSM ($j = 2$) and CGCM3 ($j = 3$) forcings. We assume that observed temperatures can be expressed as the sum of a baseline, a constant long-term trend in time, a space-time process explaining small-scale spatial and short-term temporal variability, and an observational error. The baseline captures long-range spatial variability, and it is a function of location-dependent covariates, like longitude, latitude, and elevation. RCM simulations follow a model similar to the one described above, with the addition of a model-dependent discrepancy term, that depends on location but not time. The full specification of the model is given by the equations:

$$\begin{aligned} y_t(\boldsymbol{s}) &= \boldsymbol{x}^T(\boldsymbol{s})\boldsymbol{\eta} + \xi t + \omega_t(\boldsymbol{s}) + \epsilon_t(\boldsymbol{s}), \quad t = 1, \ldots, t_0, \\ y_{jt}^{CM}(\boldsymbol{s}) &= \boldsymbol{x}^T(\boldsymbol{s})\boldsymbol{\eta} + \xi t + \omega_t(\boldsymbol{s}) + d_j(\boldsymbol{s}) + \epsilon_{jt}(\boldsymbol{s}), \quad t = 1, \ldots, t_0, \ldots, T, \end{aligned}$$

where $\epsilon_t(\boldsymbol{s}) \sim N(0, \sigma^2)$, $\epsilon_{jt}(\boldsymbol{s}) \sim N(0, \sigma_j^2)$, for $j = 1, 2, 3$, correspond to observational errors. $\boldsymbol{x}(\boldsymbol{s})$ are the k-dimensional vectors of covariates, and $\boldsymbol{\eta}$ the corresponding coefficients. ξ is the slope of the long-term temperature trend. $\omega_t(\boldsymbol{s})$ is a time and space-varying Gaussian process. $d_j(\boldsymbol{s})$ are also Gaussian processes associated with the discrepancy terms.

Following the discussion leading to Equation (1), the short range spatial variability in $\omega_t(\boldsymbol{s})$ and $d_j(\boldsymbol{s})$ is captured by representing those fields on a set basis functions with uncorrelated coefficients. Thus, taking the first M basis functions, we have that

$$\omega_t(\boldsymbol{s}) + d_j(\boldsymbol{s}) = \boldsymbol{\Psi}(\boldsymbol{s})^T(\boldsymbol{\alpha}_t + \boldsymbol{\delta}_j), \tag{2}$$

where $\boldsymbol{\Psi}(\boldsymbol{s})$ is the M-dimensional vector of basis functions evaluated at location $\boldsymbol{s}$. $\boldsymbol{\alpha}_t$ is the M-dimensional vector of time-varying coefficients. We assume that it evolves according to $\boldsymbol{\alpha}_t \sim N(\varphi\boldsymbol{\alpha}_{t-1}, \boldsymbol{\Lambda})$. $\boldsymbol{\delta}_j$ is also of dimension M and we assume that $\boldsymbol{\delta}_j \sim N(\boldsymbol{\mu}_j, \boldsymbol{\Lambda}_j)$. Here Λ and Λ_j are diagonal matrices, with elements in decreasing order. Thus we have that $\Psi_1(\boldsymbol{s})$ describes the main mode of spatial variability, $\Psi_2(\boldsymbol{s})$ the second largest mode, and so on. Correspondingly, α_{1t} is the coefficient of the main factor, α_{2t} that of the second, and so on. δ_{1j} is the coefficient for the largest mode of variability for the discrepancy of the j-th RCM, δ_{2j} the coefficient for the second largest mode, and so on.

The basis $\boldsymbol{\Psi}(\boldsymbol{s})$ is obtained using a predictive Gaussian process (Banerjee et al., 2008). This consists of defining a coarse grid over the spatial domain, considering a Gaussian process over the grid, and obtaining the predictions of this process for the rest of the domain. We then project the coefficients that provide the predictions onto the eigenvectors of the covariance matrix induced by the Gaussian process over the grid. The correlation range and the variance of the Gaussian process are unknown. They are estimated from all the data sources. Notice that the functions $\Psi_1(\boldsymbol{s}) \ldots, \Psi_M(\boldsymbol{s})$ are not orthogonal. By using a common set of bases $\boldsymbol{\Psi}$ for the baseline and the discrepancy processes, Equation (2) allows for global comparisons of the different RCM simulations. In fact, the quantification of the global differences between RCM model simulations is given by the elements of $\boldsymbol{\delta}_j$. Moreover, to estimate the common basis, all sources of information are used. Thus, the resulting estimation uncertainty reflects the variability of the observational records as well as that of the simulations.

For this application, we consider the $N \times 4$ matrix of covariates $\boldsymbol{X} = (\mathbf{1}_N, elev, lat, lon)$ where $elev$, lat and lon are N-dimensional vectors of elevations (in kms), latitude and longitude, respectively. N, the number of nodes in the RCM grid, is equal to 713. For the predictive process, we use the coarse grid configuration shown in Figure 1(a) with $M = 30$ knots and a resolution of 300 km. Following a Bayesian approach, we estimate the components of the proposed statistical model: $\boldsymbol{\eta}, \xi, \boldsymbol{\Psi}(\boldsymbol{s}), \boldsymbol{\Lambda}, \boldsymbol{\Lambda}_j, \boldsymbol{\alpha}_t, \varphi, \boldsymbol{\delta}_j, \sigma^2$ and σ_j^2, for $t = 1, \ldots, T$ and $j = 1, 2, 3$, by exploring the joint probability distribution that results from the application of Bayes theorem, after assuming a prior distribution based on prior information. We use a Markov chain Monte Carlo (MCMC) method (Gamerman and Lopes, 2006) to obtain samples from the posterior distribution of the quantities of interest. Computational details can be found in the appendix of Salazar et al. (2011).

4 Results

We show comparison and prediction results for the three different WRF simulations described in Section 2. In addition to providing insights about specific features of these simulations, this section more broadly illustrates how the presented methodology can be used to compare regional climate model simulations and to obtain blended predictions with associated uncertainty. As mentioned in the previous section, the core of our statistical model is the estimation of the seasonally varying spatial features as the basis of the comparison between ensemble members. The knowledge obtained from those comparisons is then used to obtain the blended forecasts.

Figure 3 illustrates the estimates of the spatial basis functions and their coefficients. Even though the basis functions are not orthogonal, the first row in Figure 3 show that the four largest modes capture very distinct spatial features. From the panels in the second and third rows of Figure 3 we observe that the coefficients of $\boldsymbol{\alpha}_t$ capture the interannual variability of the observations and the simulations. We can quantify the global differences between RCM simulations using the inference for the elements of the vector $\boldsymbol{\delta}_j$. The fourth and fifth rows of Figure 3 show the posterior densities of the coefficients associated with the four largest modes. Note that those coefficients are clearly separated in summer as well as in winter. This indicate that three RCM simulations considered have very distinct spatial features associated with the four largest modes of variability.

To obtain a graphical assessment of the different ensemble members over the regional domain, we estimate the discrepancy fields by computing $d_j(\boldsymbol{s}) = \Psi(\boldsymbol{s})^T \boldsymbol{\delta}_j$. Figure 4 presents such estimates for each of the three members of the ensemble. We observe that the main features in the discrepancy fields vary markedly between seasons. In the summer, there are some common features among the three forcings. There is a strong overestimation, as high as 4 °C, in most of the coastal areas in California. The CGCM3 driven pattern shows a large underestimation over most of the domain, which is to a lesser extent also present in the CCSM driven discrepancy pattern. For the winter we observe discrepancy fields that indicate markedly different behaviors for the different forcings. This can be seen in the three lower panels in Figure 4, which have few spatial patterns in common and differences of as large as 5 °C between the forcings. This is consistent with the findings by Mearns et al. (2013) that large-scale, i.e., GCM-scale, features are the dominant drivers in the winter. These distinct seasonal differences in discrepancy patterns highlight the need to compare climate models seasonally and to account for these seasonal differences in blended forecasts.

As for the temporal trend, we observe that the posterior results for ξ, the slope of the long-term temperature trend, are slightly different for summer and winter. Specifically, according to our estimations, for the 100-year time period considered (1971-2070), there is an overall predicted temperature increase of 4.2 °C (95% credible interval: 2.7–5.1) for summer and 1.8 °C (95% credible interval: 1.6–2.0) for winter.

One of the advantages of a rigorous statistical approach is the flexibility of obtaining predictions at any spatial scales while correctly accounting for the uncertainties associated with the predictions at that scale. Having this flexibility can be important to provide customized forecasts at the spatial scale that is most relevant to the needs of different stakeholders. For example, the proposed approach can provide blended predictions, with rigorously derived uncertainties, for a specific location, a state, a watershed, an ecoregion, or, more generally, for any spatial domain of interest. To illustrate this feature of the modeling approach, we show results for individual locations in four states as well as the corresponding statewide results. A comparison of the blended California summer predictions for the individual location (Figure 5) and the entire state (Figure 6) shows the scale dependency of conclusions about future climate. While the blended predictions for the state of California represent an upward correction, the blended predictions for the individual California location represent a downward correction compared to the individual simulations. This example highlights

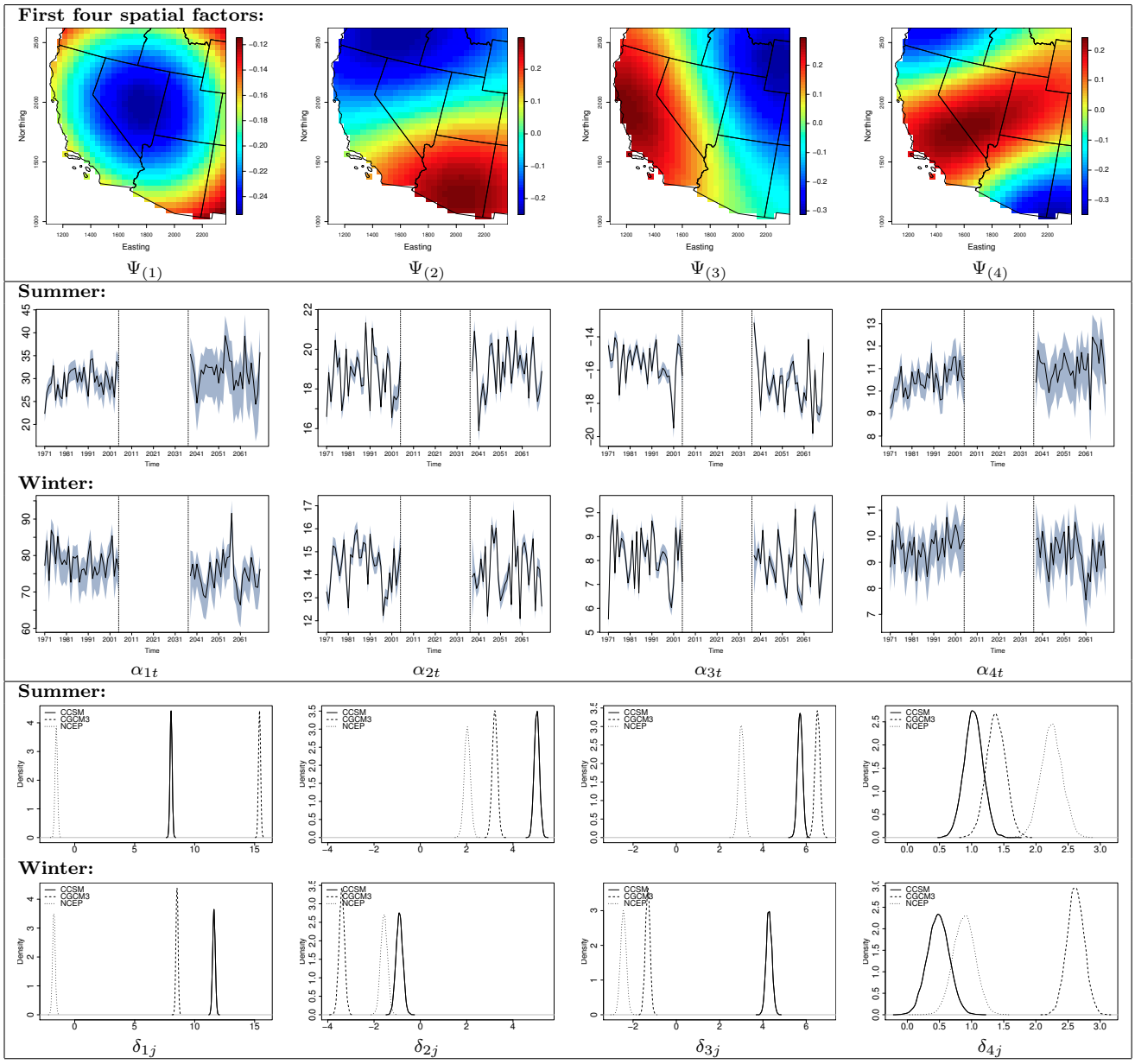

Figure 3: First row: Posterior means of $\mathbf{\Psi}_{(m)}$ associated with the first four factors. Second and third row: Time-varying coefficients α_{1t}, α_{2t}, α_{3t}, and α_{4t} corresponding to the first four factors. Black lines represent the posterior means and the gray area the 95% posterior credibility intervals. Fourth and fifth row: Posterior densities for the discrepancy coefficients, δ_{ij}, for the first four factors ($i = 1, \ldots, 4$) corresponding to NCEP ($j = 1$), CCSM ($j = 2$) and CGCM3 ($j = 3$).

how important it is to employ a blending approach that preserves the fine scale discrepancy information to aptly utilize regional climate model simulations to fulfill the needs of various stakeholders.

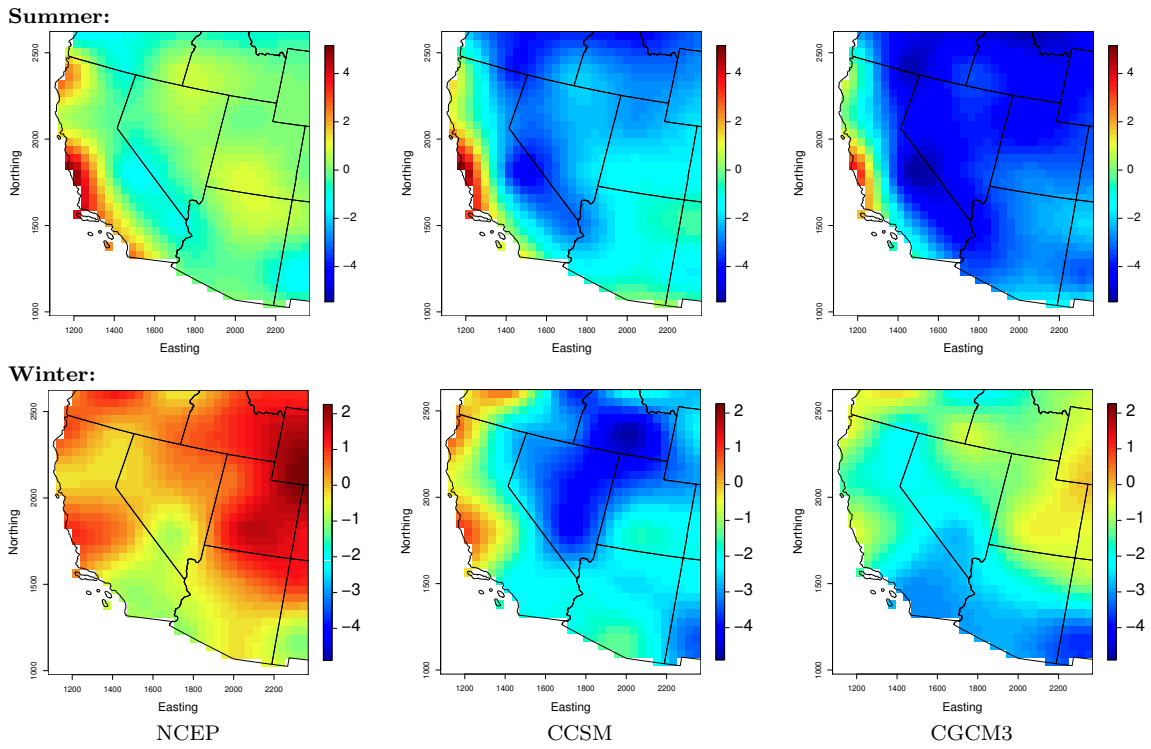

Figure 4: Discrepancies, $d_j(s)$, corresponding to NCEP ($j = 1$), CCSM ($j = 2$) and CGCM3 ($j = 3$) and for summer (1st row) and winter (2nd row), respectively.

The statewide summer predictions (Figure 6) show a clear increasing trend, with an increment between 2 and 4 °C in the 1971–2070 period. In all cases the predictions from an individual ensemble member underestimate future temperatures, when compared to blended predictions. This is not surprising, as underestimation occurs during the period under current conditions. It is important to notice, though, that the probability bands associated with the predictions are very large, showing ranges of up to 8 °C. Interestingly, even with such wide bands, some ensemble members are not fully contained within the prediction intervals and their sole use might lead to misleading conclusions. Average winter temperature predictions per state are shown in Figure 8. We observe that the increasing trend is not as pronounced as the one estimated for summer temperatures. Similarly to the summer results, we observe very wide prediction intervals and strong corrections to the RCM simulations.

A quantitative spatial assessment of temperature change between the past decade (2001–2010) and the decade from 2061–2070 is presented in Figure 9. The figure shows that overall temperatures are increasing for both summer and winter, but the spatial patterns of these increases are distinctively different between the seasons. By comparing the top and bottom panels, we observe that the change in summer temperatures is more spatially heterogeneous than the change in winter temperatures. The highest summer warming is predicted to occur in Northern Arizona, Southern Utah and Western Wyoming, with an increase of more than 2.5 °C, while the California coast, the Southeast of California and Oregon are predicted

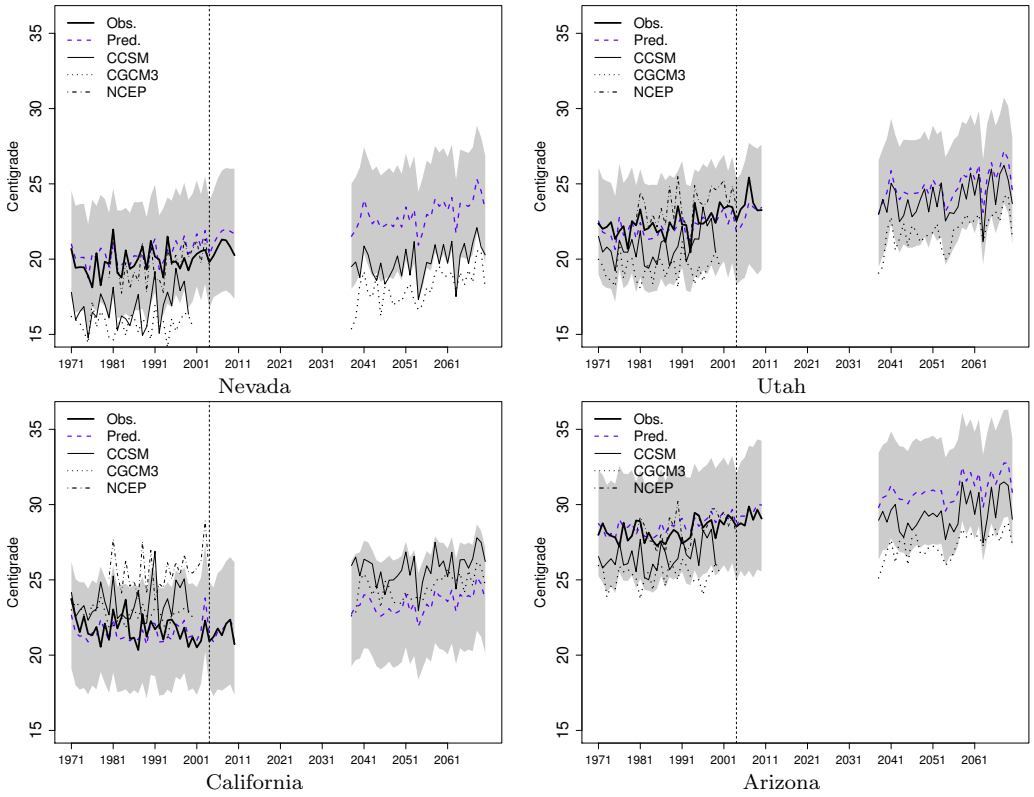

Figure 5: Times series of predictive mean **summer** temperature at four selected locations (shown in Figure 1(a)). The gray shadows correspond to 95% probability intervals.

to warm markedly less than 2 °C. Changes in the winter are more homogeneous. Most noticeable are the facts that the southern part of the California coast and the Central Valley are predicted to warm by as much as 2.6 °C. Similar levels of warming are predicted for Southern Colorado, Wyoming and Central Oregon. At the lower end, we see the border of New Mexico and Arizona, as well as some patches in Nevada and Oregon.

The Bayesian inferential framework allows valid inference to be drawn about any function of the posterior distributions. For example, the third column in Figure 9 shows the mean difference of the predictions between the two decades. We can take this even further and identify those locations where this difference exceeds some specified value at some probability level. This is illustrated in Figure 9, which shows those areas that have a 70% probability of temperature increase of at least 2 °C. Interestingly, for the investigated simulations, these areas are quite different between summer and winter. More broadly, this provides a way to incorporate the spatially varying uncertainties and translate them to tangible information for stakeholders and potentially aid in decision making under uncertainties. While a 2 °C temperature increase is a commonly used threshold for global temperature change, equivalent information can be provided for any threshold and at any spatial scale.

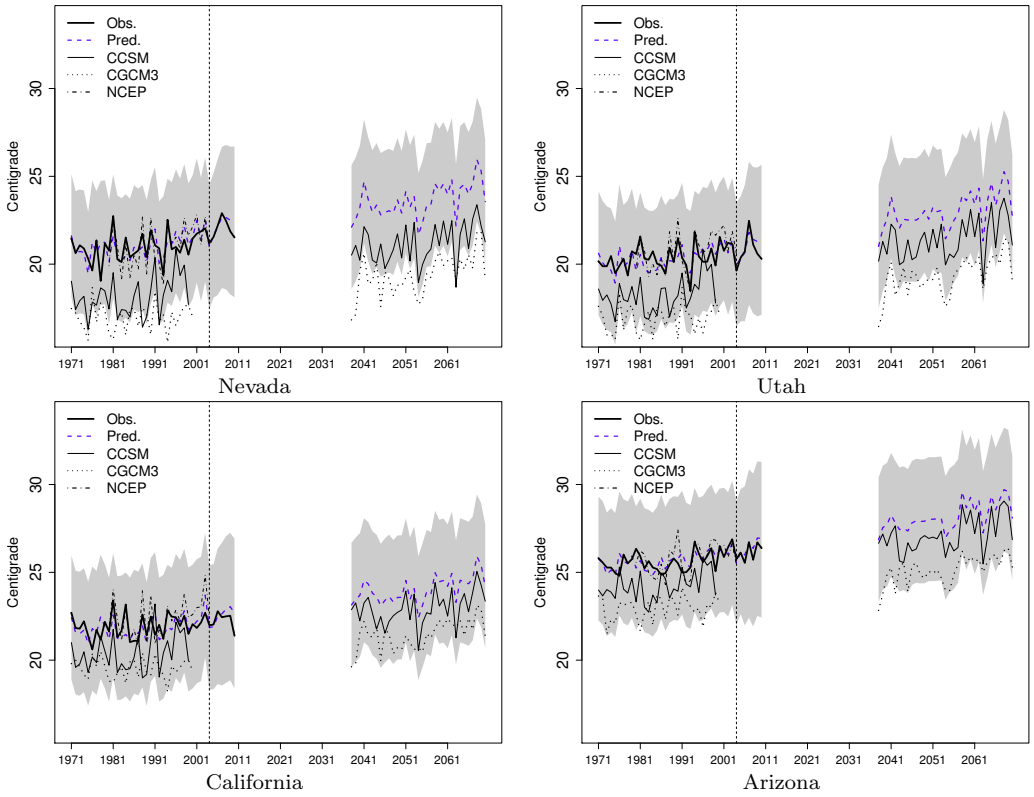

Figure 6: Times series of predictive mean **summer** temperature *averaged* by states (Nevada, Utah, California and Arizona). The gray shadows correspond to 95% probability intervals.

5 Summary and Future Work

We describe and demonstrate a methodology 1) to assess regional climate models based on their spatially varying consistency with observations and 2) to use this information to create blended projections of future climate. The methodology uses a fully Bayesian approach that provides blended projections with rigorous uncertainties. One of the advantages of the approach is the flexibility to obtain projections at any spatial scales while correctly accounting for the uncertainties associated with projections at that scale. This feature allows for creating customized blended projections with probabilistic uncertainties for any spatial domain of interest to stakeholders.

While there is no explicit weighing of models, the blended projections at a given location are based on how well, in a broad sense, a model behaved in representing past climate at that location. This can vary spatially, so the members of the model ensemble inform the blended projections in a way that is as a function of location and season. As such the methodology uses the value of regional climate models to provide high resolution information. The framework relies on the assumption that the skill of a regional climate model to describe past climate is indicative of its performance in predicting future climate. This is arguably a

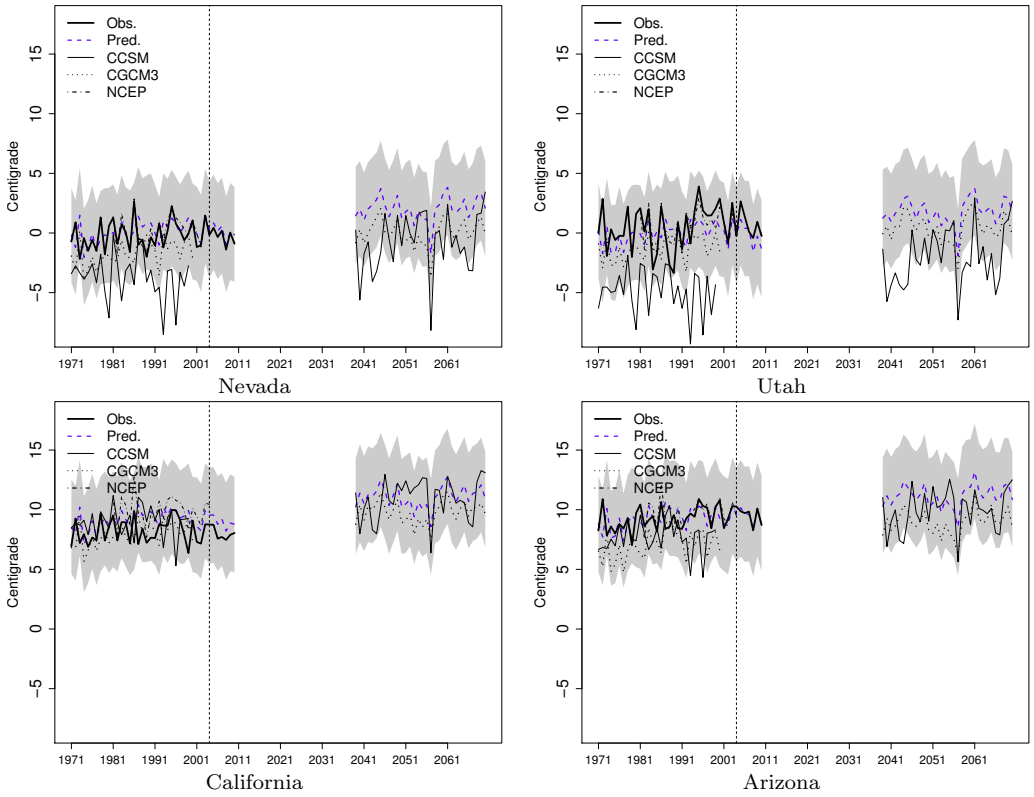

Figure 7: Times series of predictive mean **winter** temperature at four selected locations (shown in Figure 1(a)). The gray shadows correspond to 95% probability intervals.

questionable assumption, but appears preferable to ignoring any information on consistency in the past.

The analysis of the three WRF simulations and the creation of blended projections from these simulations serve as a demonstration of the methodology rather than being an attempt to create comprehensive blended projections. Nevertheless, even the analysis of such a limited ensemble highlights the importance of treating seasons differently, as discrepancy patterns vary markedly between seasons. Future work includes extending the analysis to all model runs available in the NARCCAP archive as well as future regional climate models initiatives such as the CORDEX program (Giorgi et al., 2009). Possible other extensions include assessing different variables such as precipitation.

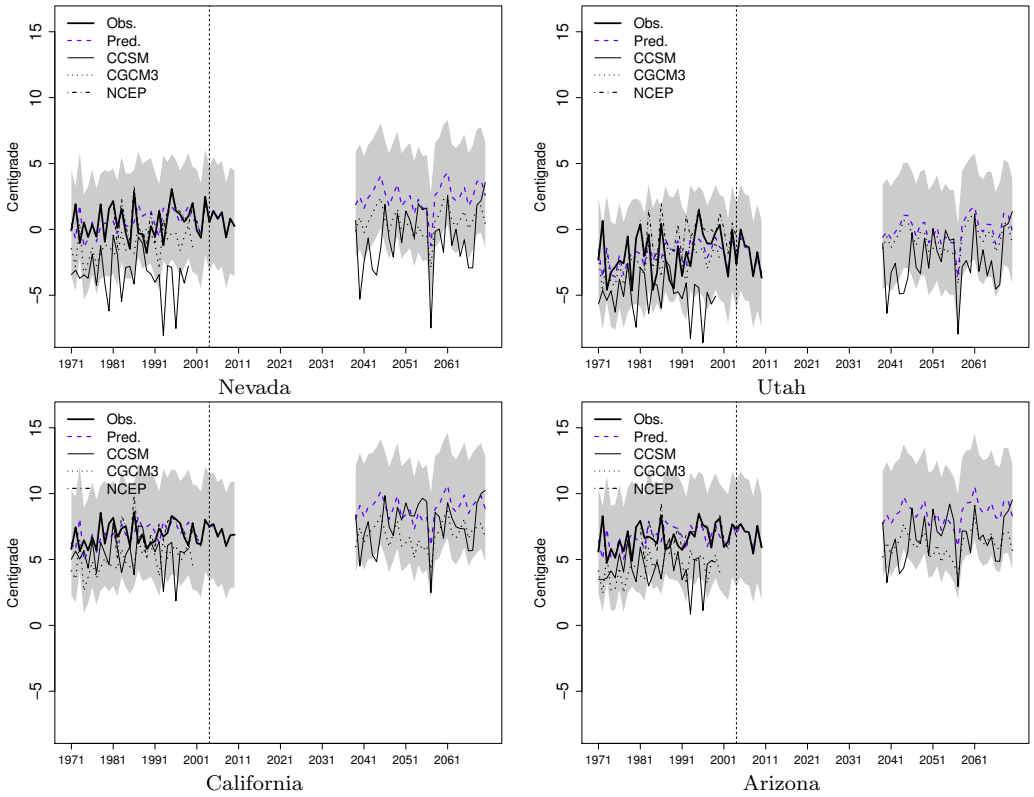

Figure 8: Times series of predictive mean **winter** temperature *averaged* by states (Nevada, Utah, California and Arizona). The gray shadows correspond to 95% probability intervals.

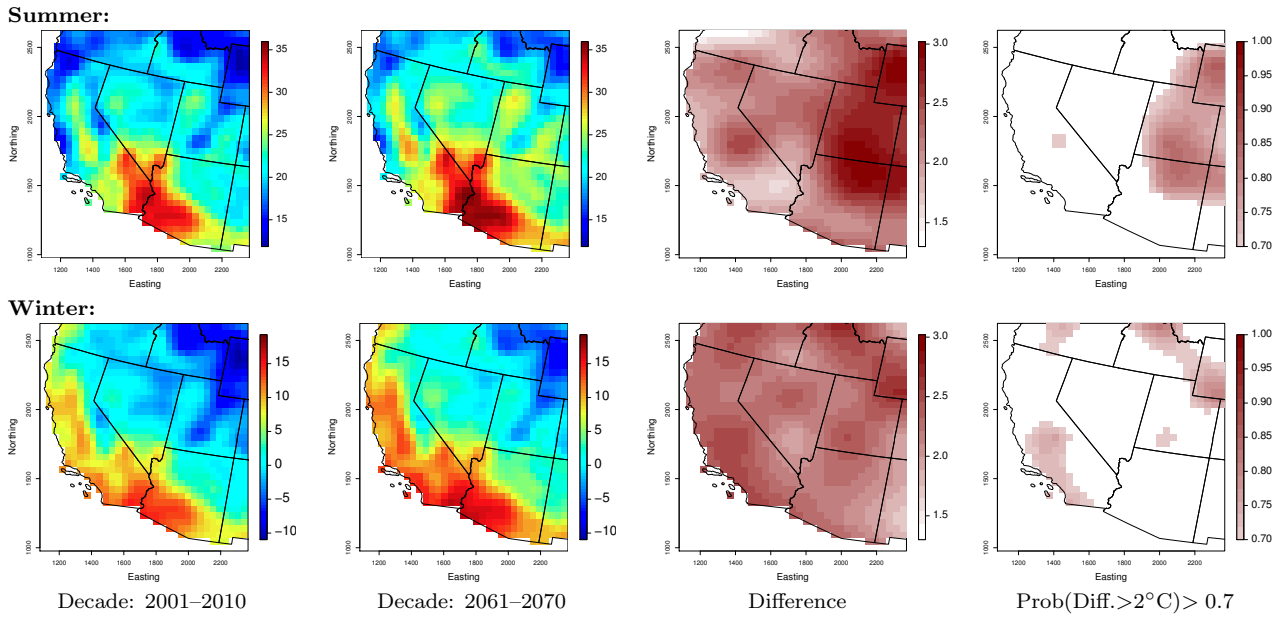

Figure 9: First and second columns: Posterior predictions for the decades 2001–2010 and 2061–2070, respectively. Third column: Difference of predictions between the two decades. Fourth columns: Probability of exceeding 2 °C difference more than 0.7. Results for summer (first row) and winter (second row).

References

Banerjee, S., Gelfand, A. E., Finley, A. O., and Sang, H. (2008). Gaussian predictive process models for large spatial data sets. *Journal of the Royal Statistical Society, B*, 70:825–848.

Beltrán, F., Sansó, B., Lemos, R., and Mendelssohn, R. (2012). Joint projections of north pacific sea surface temperature from different global climate models. *Environmetrics*, 23:451–465. DOI: 10.1002/env.2150.

Cressie, N. and Wikle, C. K. (2011). *Statistics for Spatio-Temporal Data*. Wiley, Hoboken, NJ.

Gamerman, D. and Lopes, H. F. (2006). *Markov Chain Monte Carlo - Stochastic Simulation for Bayesian Inference*. Chapman and Hall, London, UK, second edition.

Giorgi, F., Jones, C., and Asrar, G. (2009). Addressing climate information needs at the regional level: The cordex framework. *WMO Bull*, 58:175–183.

Hannachi, A., Jolliffe, I. T., and Stephenson, D. B. (2007). Empirical orthogonal functions and related techniques in atmospheric science: A review. *Int J Climatolo*, 27:1119–1152.

Mearns, L., Gutowski, W., Jones, R., Leung, L., McGinnis, S., Nunes, A., and Qian, Y. (2009). A regional climate change assessment program for North America. *EOS*, 90:311–312.

Mearns, L., Sain, S., Leung, L., Bukovsky, M., McGinnis, S., Biner, S., Caya, D., Arritt, R., Gutowski, W., Takle, E., Snyder, M., Jones, R., Nunes, A., Tucker, S., Herzmann, D., McDaniel, L., and Sloan, L. (2013). Climate change projections of the north american regional climate change assessment program (narccap). *Climatic Change*, 120(4):965–975.

Meehl, G., Covey, C., Delworth, T., Latif, M., McAvaney, B., Mitchell, J., Stouffer, R., and Taylor, K. (2007). The WCRP CMIP3 multimodel dataset: A new era in climate change research. *Bulletin of the American Meteorological Society*, 88:1383–1394.

Rougier, J., Goldstein, M., and House, L. (2010). Assessing climate uncertainty using evaluations of several different climate simulators. Technical report, Dept. of Mathematics, University of Bristol.

Salazar, E., Sansó, B., Finley, A., Hammerling, D., Steinsland, I., Wang, X., and Delamater, P. (2011). Comparing and blending regional climate model predictions for the american southwest. *Journal of Agricultural, Biological and Environmental Statistics*, 16:586–605. doi:10.1007/s13253-011-0074-6.

Smith, R., Tebaldi, C., Nychka, D., and Mearns, L. (2009). Bayesian modeling of uncertainty in ensembles of climate models. *Journal of the American Statistical Association*, pages 97–116.

Taylor, K., Stouffer, R., and Meehl, G. (2012). An overview of cmip5 and the experiment design. *Bulletin of the American Meteorological Society*, 93:485–498.

Tebaldi, C., Arblaster, J., and Knutti, R. (2011). Mapping model agreement on future climate projections. *Geophysical Research Letters*, 38:L2371. doi:10.1029/2011GL049863.

Tebaldi, C. and Sansó, B. (2008). Joint projections of temperature and precipitation change from multiple climate models: A hierarchical Bayes approach. *Journal of the Royal Statistical Society, A*, 172:83–106.